Proceedings of the Korean Nuclear Society Spring Meeting

Pohang, Korea, May 1999

Measurement of temperature profile using the infrared thermal camera in turbulent stratified liquid flow for estimation of condensation heat transfer coefficients

Sung Won Choi and Hee Cheon NO

Korea Advanced Institute of Science and Technology

ABSTRACT

Direct-contact condensation experiments of atmospheric steam and steam/air mixture on subcooled water flowing co-currently in a rectangular channel are carried out using an infrared thermal camera system to develop a temperature measurement method.
The inframetrics Model 760 Infrared Thermal Imaging Radiometer is used for the measurement of the temperature field of the water film for various flow conditions.
The local heat transfer coefficient is calculated using the bulk temperature gradient along the flow direction. It is also found that the temperature profiles can be used to understand the interfacial condensation heat transfer characteristics according to the flow conditions such as noncondensable gas effects, inclination effect, and flow rates.

1. Introduction

Direct contact condensation is fundamentally important in LWR safety analysis and other industrial applications. Especially, during a postulated LOCA(Loss Of Coolant Accidents), cold ECCW(Emergency Core Cooling Water) would be injected to cool down the reactor core. When the subcooled water is injected into the horizontal pipe filled with steam, the steam flows over the water in the opposite direction and steam condensation occurs in a stratified flow. The local condensation rate and the relative motion of steam and water are important in the determination of core uncovery. Furthermore the local condensation heat transfer coefficients are the key parameter of water hammer. (S.J. Kim 1996) Especially, for the case of thin water layer flow, Segev et al(1981) evaluated the interfacial condensation heat transfer coefficient from an increases in the bulk temperature of water flow. They measured the temperature of the water-side wall surface which were used as a bulk temperature of water flow. And this seems to be reasonable in cases there were not great differences between the

bulk temperatures of water flow and the wall surface temperatures for the water flow. However, in order to get the accurate local condensation heat transfer coefficients, it is necessary to measure the temperature profile without any flow disturbance in getting the local heat transfer coefficient.

2. Experimental works

2.1 Description of an experimental loop

An adiabatic two-phase loop is modified to carry out direct-contact condensation experiments. The overall schematic diagram of the experimental facility is shown in Figure 3.1.

Several variables are measured to obtain a direct-contact condensation heat transfer coefficient. In the test loop, the flow rate, pressure, and temperature of mixture in the test section are locally measured. The inlet pressure and temperature in the test section are measured at the top of the water vessel connected to the test section. Water subcooling is controlled based on the temperature measured in the water vessel. Inside the test section, local bulk mean temperatures are measured by thermocouples and the infrared thermal camera at two locations.

2.2 Temperature measurement system

In order to measure the temperature profile and visualization of the temperature field, two infrared glasses are specially installed, which are parallel to the inside surface of the side wall of the test section in order to make disturbances in the water flow as small as possible.

As seen figure 3.3, the first one is located 72cm away from the entrance of the test section for the purpose of visualization of the interface of stratified flow. Therefore, the infrared glass is located 5mm above the bottom of the wall. The other one is located 122cm away from the entrance of the test section in order to measure the temperature profile to get the bulk temperature. For cross-checking the temperature measured by the infrared thermal camera, T-type thermocouples with a thickness of 1mm are installed at the side wall in the vertical direction at the 0.4mm regular intervals between thermocouples. The detailed diagram of the installed infrared glasses and thermocouples is shown in figure 3.2.

2.3 Infrared Thermal camera systems

This system has the advantage of being noninvasive, thus allowing measurements without interfering with environments under investigation. It also maps continuously the entire region of interest. The output can be displayed on a video screen, thus permitting real-time evaluation of the result. The detailed diagram of the infrared thermal camera system is shown in figure 3.3.

3. RESULTS AND DISCUSSION

3.1 Local heat transfer coefficient

To evaluate the mean temperature and velocity at each vertical position from the bottom, the temperature and velocity profiles in the cross-sectionally horizontal direction are assumed as follows:

(a) The temperature profile is uniform in the cross-sectionally horizontal direction.

(b) The velocity profile follows the law of the wall in the cross-sectionally horizontal direction. From the energy balance equation the heat transfer coefficient is defined as follows:

$$h_z = \frac{C_{pL} \cdot W_L(z)}{b[T_G - T_L(z)]} \cdot \frac{dT_L(z)}{dz} \quad . \tag{1}$$

Universal velocity profiles from the law of the wall are as follows:

$$u_w^+ = y_w^+ \quad , \quad \text{for} \quad y_w^+ < 5 \quad , \tag{2}$$

$$u_w^+ = 5.0 \ln y_w^+ - 3.05 \quad , \quad \text{for} \quad 5 < y_w^+ < 30 \quad , \tag{3}$$

$$u_w^+ = 2.5 \ln y_w^+ + 5.5 \quad , \quad \text{for} \quad y_w^+ > 30 \quad , \tag{4}$$

where $u_w^+ = \bar{u} / u_\tau$, $y_w^+ = y_w \cdot u_\tau / \nu$, and $u_\tau = \sqrt{\tau_w / \rho}$,

$\frac{\tau_w}{\rho} = \frac{c_f u_\infty^2}{2} = u_\tau^2$, and $c_f \approx 0.0791 \, Re_D^{-1/4}$ for $4000 < Re_D < 10^5$.

The bulk liquid temperature is defined as follows:

$$T_L = \frac{\int T_{L,mean}(y) \cdot V_{L,mean}(y) \cdot dy}{\int V_{L,mean}(y) \cdot dy} \quad , \tag{5}$$

where $V_{L,mean}(y)$ and $T_{L,mean}(y)$ are the mean velocity and mean temperature across the channel width. $V_{L,mean}(y)$ is calculated from the assumption of the law of the wall and $T_{L,mean}(y)$ is equal to $T_{L,center}(y)$, as shown in figure 3(a).

In order to evaluate the applicability of the IR thermal camera to calculate the heat transfer coefficient, the temperatures measured by thermocouples and the IR thermal camera are compared. The first step is the comparison of temperature from the thermocouples and the IR thermal camera one. The second one is to compare the center temperatures directly measured by the traversing thermocouple in the water layer with wall one measured by thermocouples installed in the wall. The third one is to compare the temperature profile measured by the thermocouple traversing in the water layer with the one measured by IR thermal camera in the same width direction of the wall side of the test section. For the case of the first one it

is found that the IR thermal camera can measure the temperatures with an error bound of ± 0.5℃ as we can find the same result from the lots of previous works of IR imaging experiments. In the second one, Fig 3(a) shows that temperature profiles between the center temperature directly measured by traversing the thermocouple in the middle of width and the wall temperature measured by thermocouples installed in the wall are almost the same. The result of the third step of experiments is shown figures 3(b) which is the IR thermal imaging picture. There is 1% of temperature difference between them.

Finally, we apply this measurement method to get the bulk temperature profile using the velocity information from the law of the wall. The results of the experiments are shown in figures 4(a) and 4(b). In figure 4(a), Rbt1 and Rt1 indicate the temperatures measured by thermocouple located in the middle of the channel. The infrared thermal camera is positioned at the same distance of Rt1 so as to cross-check the temperature. Flow condition is cocurrent with 5° in inclination and 62℃ in inlet water temperature. The rest of the information are shown in Fig. 4(a). The calculated heat transfer coefficient(HTC) is compared to one produced from the same experimental conditions performed by Choi(1998). The developed method produces less local heat transfer coefficient than that estimated by using the bottom wall temperatures. That is because the bulk mean temperature using the bottom wall temperature is smaller than that calculated by using both the temperature profile measured by the infrared thermal camera and the law of the wall.

3.2 Visualization of temperature field

Heat transfer phenomena are explained with parameters related to visualization of the temperature field such as temperature difference between the mean temperature and the interface water layer temperature, the clearness of the isothermal boundary line and the temperature profile gradient. In figure 5 it is explained about how to read infrared thermal pictures for the temperature profiles of the various flow conditions. The image of the temperature field data can be saved in real time and the analysis of the temperature field are performed with various software tools. One of them is to draw the line between two interesting points in the temperature field. Then the temperature gradients between two points can be obtained.

3.3 Cocurrent flow

3.3.1 Effects of steam flow rate

The interface of the water layer is stable for the low steam flow rate as shown in figure 6(a). Figure 6(c) shows that the interface of water flow becomes wavy as the steam flow increases because the temperature profile line fluctuates. When the steam flow rate becomes very large, an agitation with the high frequency and the small amplitude occurs in the

interface, which increases the heat transfer rate. The temperature field perturbation is increased as the steam flow rate increases. Figures 6(a) through 6(c) show that the temperature difference between the water temperature of the bottom side and the interface of water decreases rapidly, which means the heat transfer rate increases as the steam flow rate increases.

3.3.2 Effects of inlet water temperature

Figures 6(d) and 6(e) show that temperature profiles become steep as the inlet water temperature increases. It is also found that in case the temperature difference between the bottom and the top of the water layer decreases the large perturbation of the temperature field is observed, which induces an increase in the heat transfer rate. For the high inlet water temperature, the effects of steam flow on interfacial heat transfer are similar to those of results as shown in figures 6(a) and 6(c).

3.4 Countercurrent flow

The similar phenomena to the counter-current flow are observed for the effect of steam flow rate and inlet water temperature in cocurrent flow . To compare figure 6(d) with figure 7(b), heat transfer in cocurrent flow is more enhanced than that of countercurrent flow because the temperature difference between the mean temperature and the top of water layer temperature in countercurrent flow is larger than cocurrent one.

Figures 7(a) and 7(c) show that temperature profiles become steep as the inlet water temperature increases. It is also shown that heat transfer near the interface of water increases as the inlet water temperature increases.

3.5 Countercurrent flow with non-condensable gas

The big difference between the pure steam flow and the steam with noncondensable gas is the temperature at the top of water layer. Due to the noncondensable gas nearby interface of water layer gas temperature profile decreases as the mass fraction of noncondensable gas increases as shown figures 8(a) and 8(b). That must be an important point in heat transfer because of the heat resistance layer thickness owing to the noncondensable concentration. Inlet water temperature effects are similar to other cases as shown in figures 8(a) and 8(b).

3.6 Flow visualization of temperature field

It has been known that the heat transfer rate increased along with an inclination of water flow due to the fact that high wave amplitude helps the increase of the surface renewal rates. In figure 10, the direction of the waves motion is opposite to the flow direction by the force of the shear stress of high steam flow. That makes the entrainment of the waves which induce the active heat transfer between the gas mixture and subcooled liquid flow. However, the flow condition reaches the countercurrent flow limit quickly.

4. CONCLUSIONS

The inframetrics Model 760 Infrared Thermal Imaging Radiometer is used for the measurement of the temperature profile and the temperature field of the water flow according to the flow conditions at the experimental works. The main findings are as follows:

(a) The temperature difference measured by between the thermocouples and the infrared thermal camera is less than ±0.5℃ for the same height. So we assume that the temperature profiles are uniform along with width direction of the water layer.

(b) The temperatures measured by infrared thermal camera are calibrated by the thermocouples and the temperature profiles measured by the thermocouples shows almost the same with those measured by the infrared thermal camera. And then the local heat transfer coefficient is calculated by using the bulk temperature profile measured by the infrared thermal camera.

(c) The temperature field patterns especially temperature gradient in the water layer according to the flow conditions such as the flow directions (countercurrent or cocurrent), the inclination degree and the inlet water temperature can be used to understand the interfacial condensation heat transfer characteristics.

In all cases it is found that the temperature profiles become uniform, which means that the wide mixture isothermal layer nearby interface is shown as the inlet water temperature increases. When the ratio of noncondensable gas is increased, the temperature of interface water layer becomes much less than the saturated temperature even though wave amplitude increases. The inclination degree has an important role in increasing wave amplitudes which increase the surface renewal rates.

References

[1] G. Hetsroni, A. Mosyak and L. P. Yarin, "Effect of surface waves on heat transfer in natural and forced convection," Int. J. Heat Mass Transfer, Vol. 40, No. 9, pp. 2219-2229, 1997

[2] G. Hetsroni, L. P. Yarin and D. Kaftori, "A mechanistic model for heat transfer from a wall to a fluid," Int. J. Heat Mass Transfer, Vol. 39, No. 7, pp. 1475-1478, 1996

[3] K.Y. Choi "Direct-contact condensation heat transfer with noncondensable gases and interfacial shear for co-current stratified wavy flow in nearly-horizontal channels" PhD. thesis, KAIST, 1998

[4] G. Hetsroni, R. Rozenblit and D. M. Lu, "Heat transfer enhancement by a particle on the bottom of a flume," Int. J. Multiphase Flow Vol.21, No. 6, pp. 963-984, 1995

[5] H.J. Kim, "Local properties of countercurrent stratified steam-water flow," PhD. thesis, Northwestern Univ. Evanston, Illinois, 1983

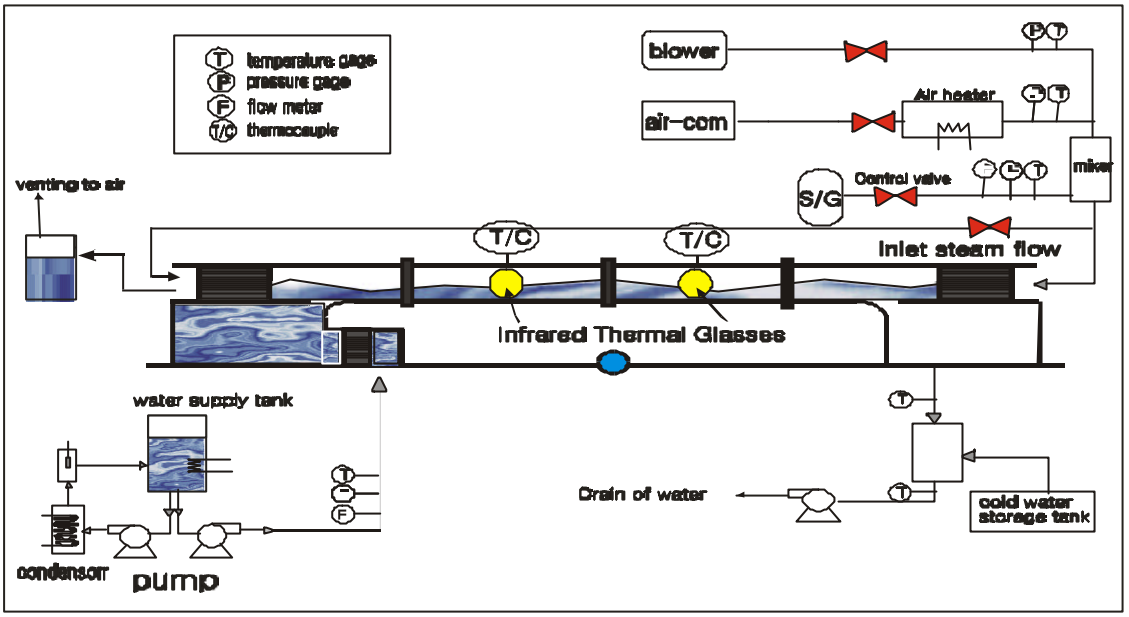

Fig 1. Experimental facility

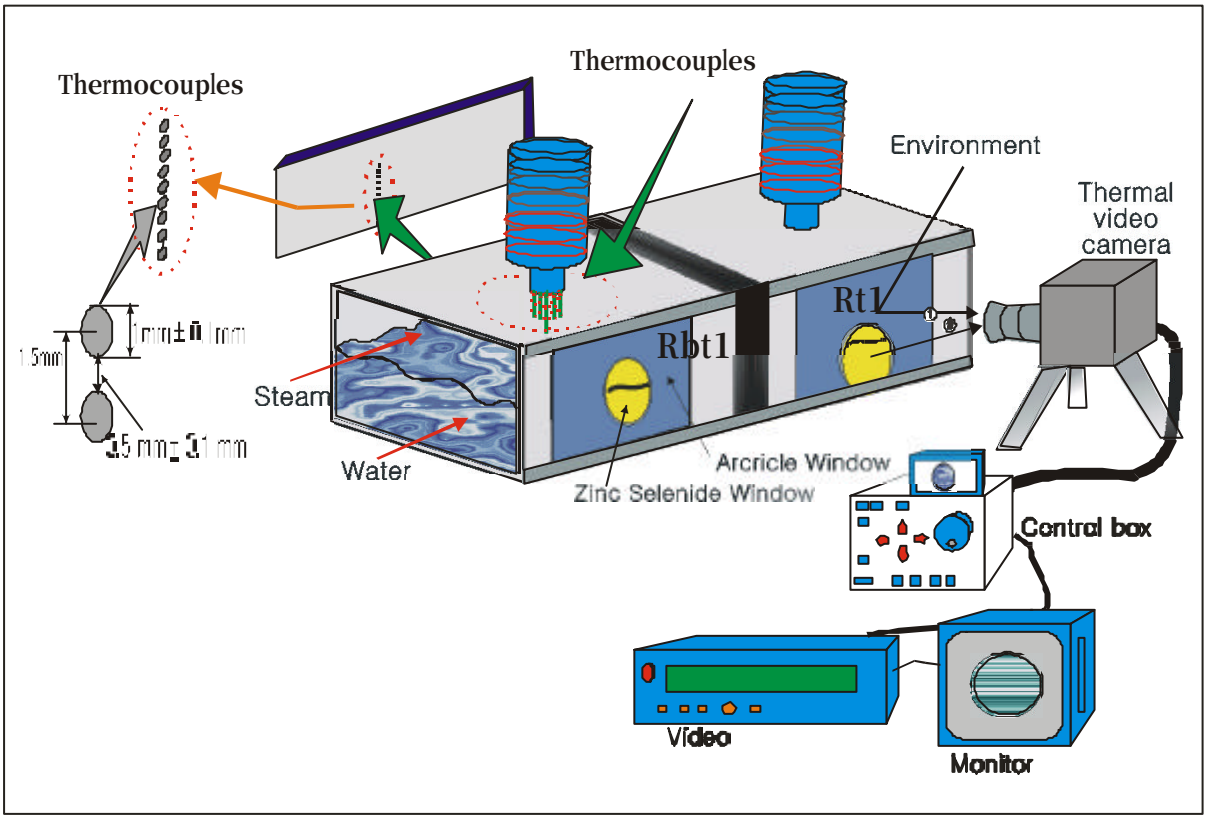

Figure 2. Temperature measurement system

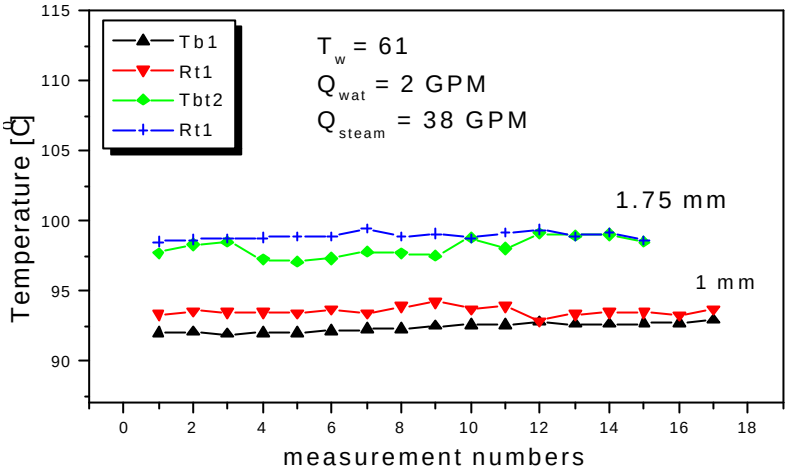

(a)

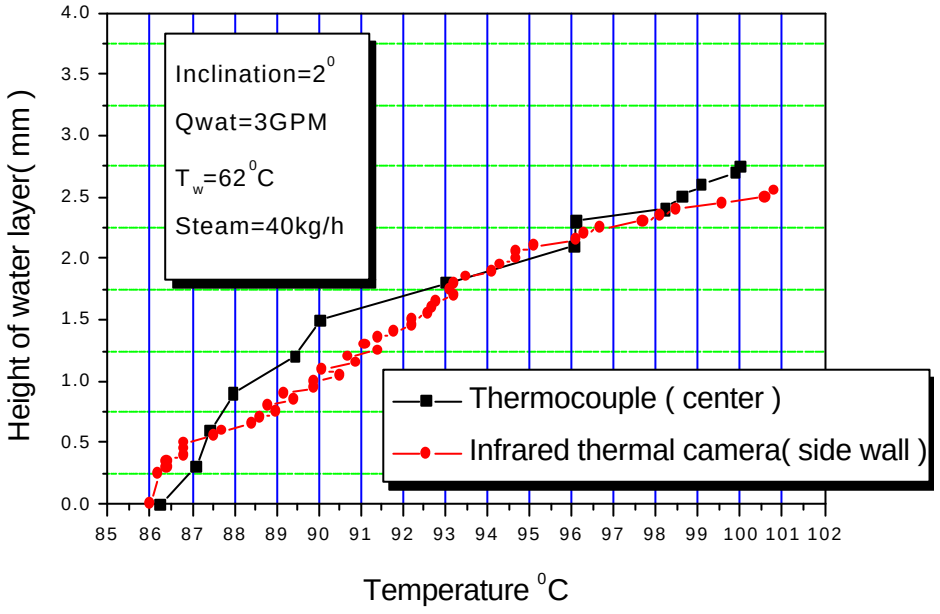

(b)

Figure 3. Temperature profile calibration

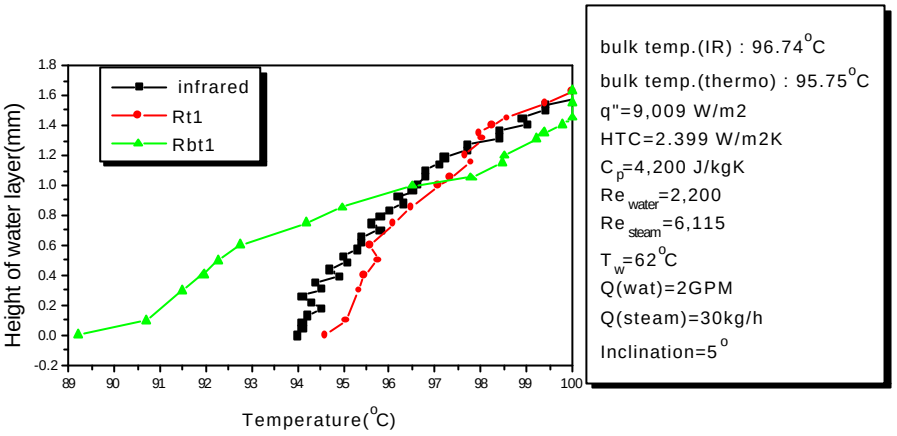

(a)

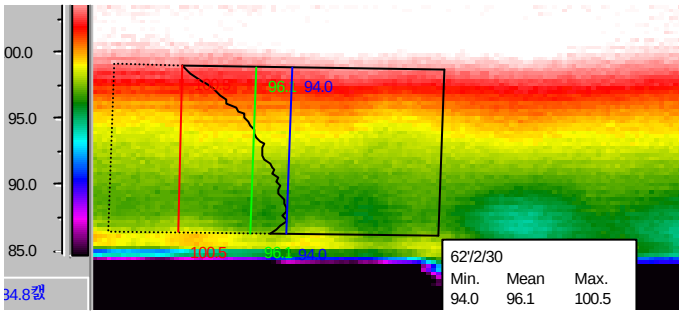

(b)

Fig 4. Calculation of heat transfer coefficient

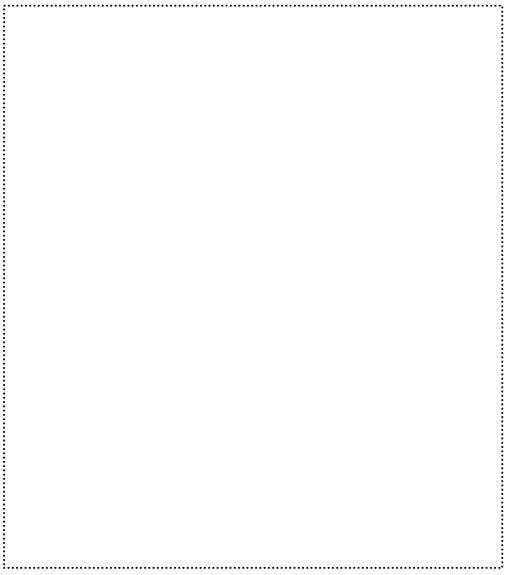

(a) 63-3-40-2.75means as flollows:

$T_{fin} = 62\,℃,\ m_f = 3GPM,\ M_s = 40kg/hr$

water layer thickness = 2.75 mm

(b) Reference temperature bar

(c) Minimum temperature line

(d) Mean temperature line

(e) Maximum temperature line

(f) Edge point of temperature profile

(g)Beginning point of temperature

(h) Frame of infrared glass

(i) Position of temperature measurement

Fig 5. Explanation of infrared thermal picture

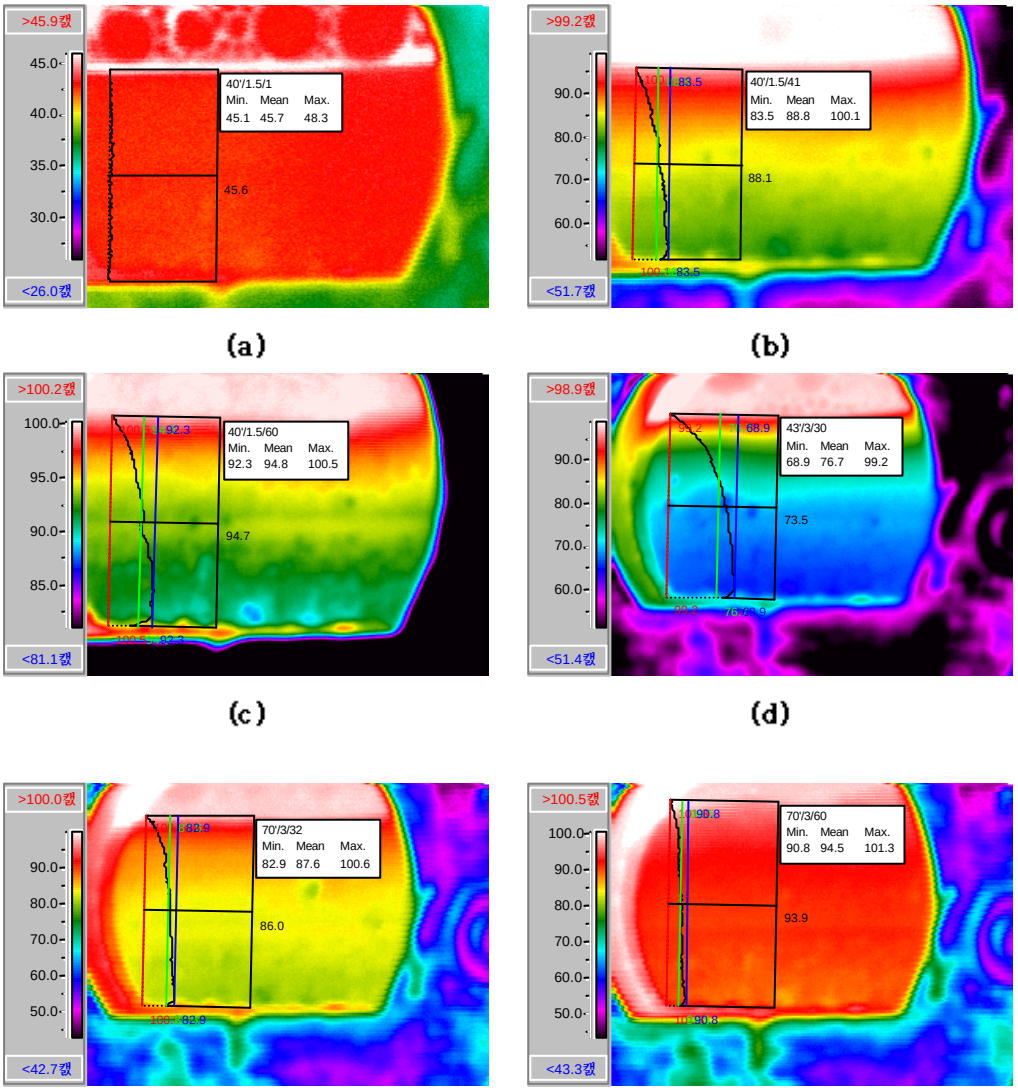

Figure 6. Temperature profile of horizontal cocurrent flow

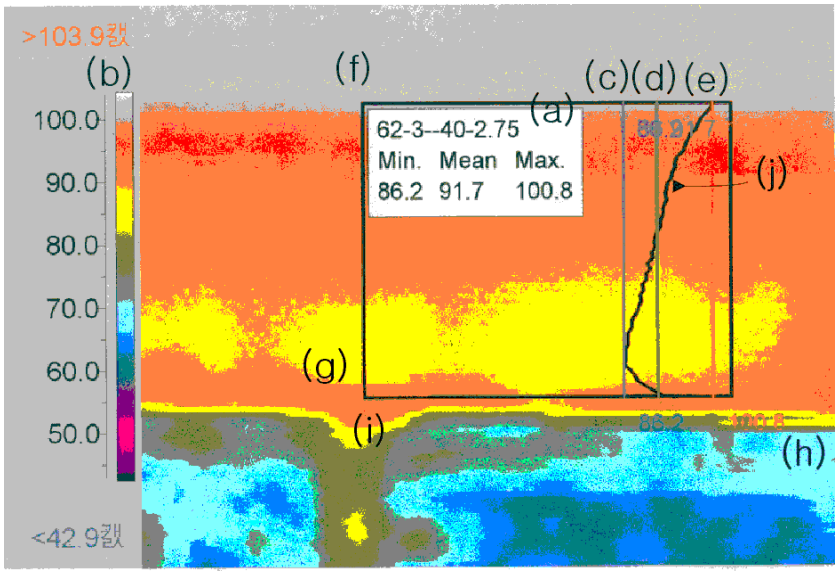
>103.9캘
(b)
(f)
(c)(d)(e)
(a)
100.0
90.0
80.0
70.0
60.0
50.0
62-3--40-2.75
Min. Mean Max.
86.2 91.7 100.8
(j)
(g)
(i)
(h)
<42.9캘